2320

Temperature Distribution in a Circulating Drilling Fluid

L. R. Raymond, SPE-AIME, Esso Production Research Co.

Introduction

With the trend toward deeper and consequently hotter holes, measurements of drilling mud properties at atmospheric temperatures are becoming increasingly inadequate.[1] Both the prediction and control of downhole mud properties depend in part upon our knowledge of temperatures in the wellbore. Consequently, a better understanding of factors that affect temperatures during circulation and trips could improve drilling operations. It was toward the goal of obtaining this understanding that this study was directed.

Other investigators[2] have studied the response of fluid temperature in the borehole during trips. However, all of these studies have used an assumed formation temperature profile at the conclusion of circulation and have provided no means to calculate this profile directly. In this study, the formation profile during circulation was calculated. Other investigators[3-5] have also studied bottom-hole temperature during circulation. However, they have developed neither general techniques for calculating the entire temperature profile in the system nor generalized methods for predicting bottom-hole fluid temperatures during circulation. Such techniques and methods have been developed and are discussed briefly in the following pages.

Temperature Behavior During Circulation

Circulation of fluid during the drilling operation is represented schematically in Fig. 1. The process of circulation has three distinct phases: (1) fluid enters the drill pipe at the surface and passes down the drill pipe; (2) fluid exits the drill pipe through the bit and enters the annulus at the bottom; and (3) fluid passes up the annulus and exits the annulus at the surface. To simulate the thermal behavior of the fluid in the system, each of the phases of circulation must be described mathematically.

In Phase 1, the fluid enters the drill pipe at a specified temperature, T_{Do}. As the fluid passes down the pipe, its temperature is determined by the rate of heat convection down the drill pipe, the rate of heat exchange between the drill pipe and the annulus, and time. Phase 2 of the circulating process merely requires that the fluid temperature at the exit of the drill pipe be the same as the fluid temperature at the entrance of the annulus; i.e., $T_D(L, t) = T_A(L, t)$. Thus in Phase 3, the fluid enters the annulus at $T_D(L, t)$. As the fluid flows up the annulus, its temperature is determined by the rate of heat convection up the annulus, the rate of heat exchange between the annulus and the drill pipe, the rate of heat exchange between the formation adjacent to the annulus and the fluid in the annulus, and time. These rates of heat exchange and the time dependency of mud temperature are described by well known heat-flow equations.[6] Consequently, as shown in the Appendix, the temperature profiles in the drill pipe, annulus, and formation can be obtained by solving Eqs. 1 through

A technique for calculating drilling temperature as a function of position and time shows that circulation lowers considerably the temperatures of both the bottom-hole fluid and the rock and that the maximum circulating fluid temperature occurs a fourth to a third of the way up the annulus.

3 with the additional requirement specified by Eq. 4, once appropriate initial and boundary conditions are specified.

$$A_D\, \rho v_D\, C_p \frac{\partial T_D(Z,t)}{\partial Z} + 2\pi r_D\, U\, [T_D\,(Z,t) - T_A\,(Z,t)] = -\rho A_D C_p\, \frac{\partial T_D(Z,t)}{\partial t}, \quad . \quad (1)$$

$$A_A\, \rho v_A\, C_p \frac{\partial T_A(Z,t)}{\partial Z} + 2\pi r_D\, U\, [T_D\,(Z,t) - T_A\,(Z,t)] + 2\pi r_B\, h_f\, [T_f(r_w, Z, t) - T_A\,(Z,t)] = \rho A_A\, C_p \frac{\partial T_A\,(Z,t)}{\partial t}, \quad . \quad (2)$$

$$\frac{\partial T_f(r_w, Z, t)}{\partial t} = \frac{k_f}{\rho_f\, C_{pf}}\, \frac{1}{r}\, \frac{\partial}{\partial r}\left[r\, \frac{\partial T_f(r_w, Z, t)}{\partial r}\right], \quad \dots \quad (3)$$

$$2\pi r_B\, h_f\, [T_f(Z,t) - T_A(Z,t)] = 2\pi r_B\, k_f \left[\frac{\partial T_f(Z,t)}{\partial r}\right]_{r=r_B} \quad \dots \quad (4)$$

Unsteady State Solution

In field situations, the mud's inlet temperature to the drill pipe is generally available through direct measurement. Hence, the boundary condition for Eq. 1 is $T_D\ (Z{=}0,\, t) = T_{Do}\ (t)$. From previous considerations it has already been established that $T_D\ (Z{=}L, t) = T_A\ (Z{=}L, t)$, and this will serve as the boundary condition for Eq. 2.

When circulation is started following a trip, the fluid temperature in the borehole has approached the geothermal temperature of the adjacent formation. In this study, it will always be assumed that the geothermal temperature is given by $a + bZ$, where a is the surface formation temperature, and b is the geothermal gradient. The initial distribution of fluid temperature in the drill pipe and annulus is given by the geothermal temperature; that is, $T_D\ (Z, t) = T_A\ (Z, t) = a + bZ$. Similarly, the initial temperature for the formation at a given depth is assumed to be uniform and at the same level as the geothermal temperature.

One boundary condition for Eq. 3 requires that the flux out of the formation be the same as the flux into the annulus and is given by Eq. 4. Since at large values of r the geothermal temperature is undisturbed, the second boundary conditions is: $T_f\ (r \rightarrow \infty, Z, t) = a + bZ$. With these boundary and initial conditions, Eqs. 1 through 3 were solved numerically to obtain the transient temperature profiles for the circulating fluid system. The solutions are obtained by the procedure described in the Appendix.

The solutions obtained are surfaces in the three dimensions of depth, time and temperature. Consequently, there are several methods to present the results of the calculations. In Fig. 2, the three most important temperatures — outlet, bottom-hole fluid, and bottom-hole formation — are plotted as a function of time. The well simulated to obtain these results was a 20,000-ft well with an 18 lb/gal oil-base mud being circulated at 200 gal/min. The geothermal gradient was 1.6F/100 ft and the surface formation temperature was 80F. Inlet temperature was held constant at 135F during the entire 16 hours of circulation.

As Fig. 2 shows, the calculated outlet temperature rises rapidly from 80 to 147F and then reaches an almost constant level at 148F. In the last 9 hours of circulation, the outlet temperature changed 1°F. In any field situation this change would be imperceptible. The bottom-hole fluid and bottom-hole rock temperatures fell very rapidly from their initial value of 400F (geothermal bottom-hole temperature) following the start of circulation. A constant temperature difference between the bottom-hole fluid and rock is set up almost immediately and maintained throughout the life of the circulation process. The important point to note with respect to the bottom-hole fluid temperature is that it continually changes with time; a steady-state condition is never attained. This time-

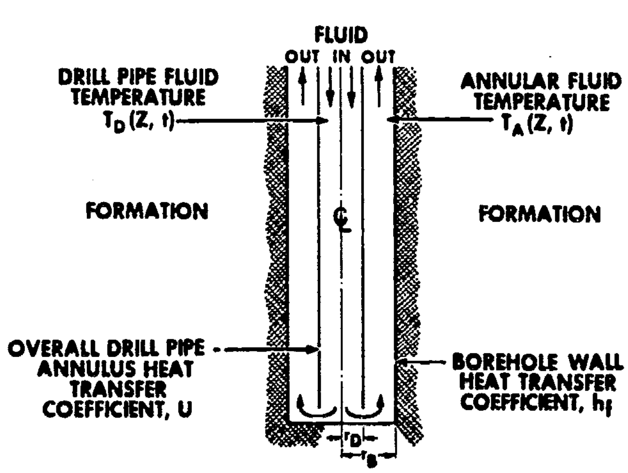

Fig. 1—Schematic of circulating fluid system.

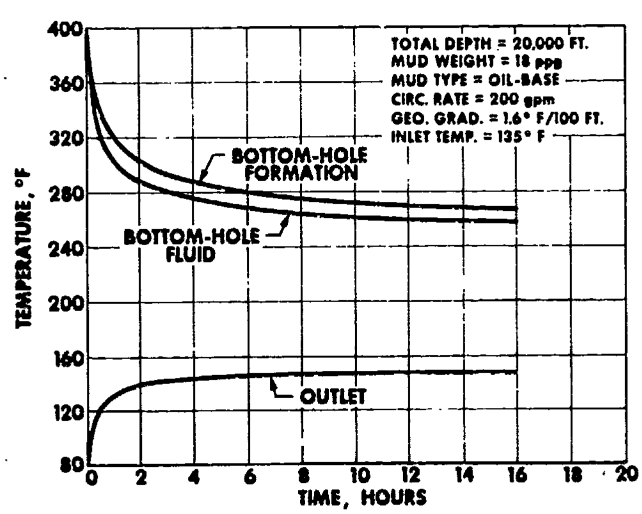

Fig. 2—Effect of time on temperature for a simulated well.

dependence of bottom-hole fluid temperature takes place even though both the inlet and outlet temperatures are held constant. Hence the stabilization of both inlet and outlet temperatures does not mean that all of the temperatures in the circulating system are constant.

Fig. 3 shows temperature as a function of depth for the same system at 2 hours of circulating time. Note that the over-all effect of circulation has been to heat the formation between the surface and 12,000 ft and to cool the formation from 12,000 to 20,000 ft. Also there is a reversal in the temperature differential between annular fluid and borehole wall at 10,000 ft so that the formation above 10,000 ft is being heated and the formation below 10,000 ft is being cooled at this particular circulation time. It is also important to note that the maximum fluid temperature does not occur at the bottom of the hole but rather in the annulus, after the fluid has made the turn at the bottom and is exposed to the high formation temperature. In our case, the maximum fluid temperature occurs at 17,000 ft. This point will tend to move up as circulation time increases. It usually establishes itself at approximately one-fourth to one-third of the way up the annulus. The location of the maximum temperature point is dependent on circulating velocity; it moves up the annulus as circulating velocity increases.

The profiles in Figs. 4 through 6 give the calculated history of the drill-pipe fluid, annular fluid, and borehole wall temperature. These curves represent the dynamic response of the system.

Pseudo-Steady State Solution

Examination of the results of several sets of calculations indicated that shortly after the "bottoms come up" the thermal behavior of a mud system begins to approach a slow, logarithmic decline. Such a decline suggests that diffusion of heat into or out of the formation is a controlling factor. In this case the unsteady state terms in Eqs. 1 and 2 become negligible, and the equations describing the system are

$$A_D \rho v_D C_p \frac{dT_D(Z)}{dZ} + 2\pi r_D U\,[T_D(Z) - T_A(Z)] = 0 \quad , \; . \; . \; . \; . \; . \quad (5)$$

and

$$A_A \rho v_A C_p \frac{dT_A(Z)}{dZ} + 2\pi r_D U\,[T_D(Z) - T_A(Z)] + 2\pi r_B h_f\,[T_f(t, Z) - T_A(Z)] = 0 \; . \; . \quad (6)$$

The dependence of temperature on time is now introduced only through the formation temperature, which is still represented by the radial diffusion equation. In the unsteady state case the equations for T_D and T_A were solved analytically in terms of the borehole wall temperature $T_f(t, Z)_{r=r_B}$. (See Appendix.) The explicit relationships for T_D and T_A as functions of Z at a given time t are

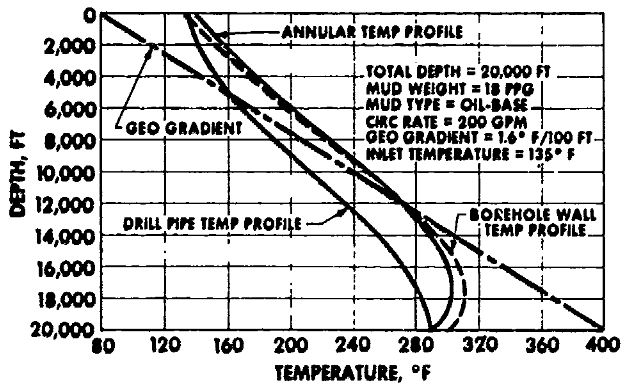

Fig. 3—Temperature as function of depth at 2 hours of circulation time for a simulated well.

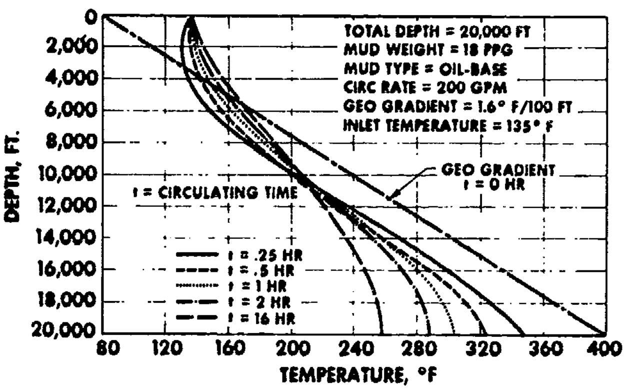

Fig. 4—Drill pipe temperature vs depth as a function of time for a simulated well.

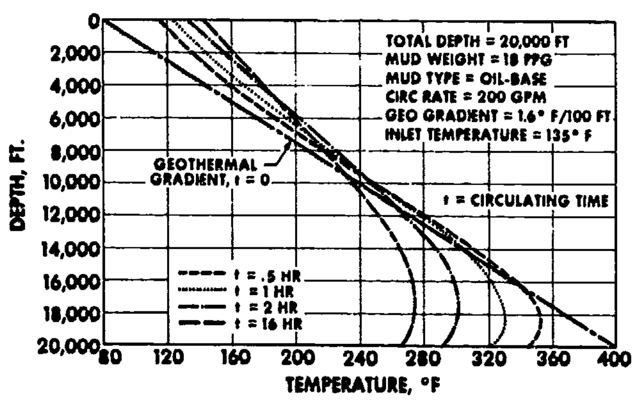

Fig. 5—Annulus temperature vs depth as a function of time for a simulated well.

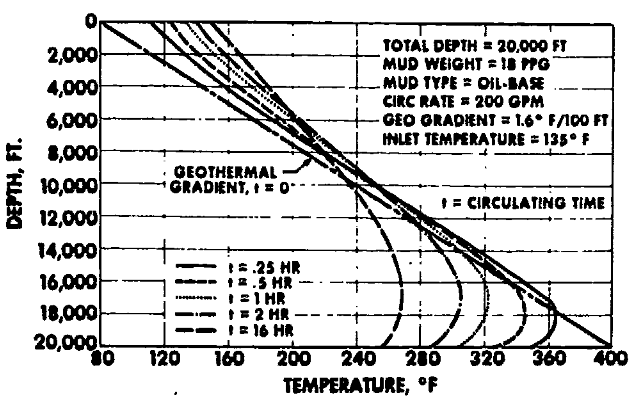

Fig. 6—Borehole wall temperature vs depth as a function of time for a simulated well.

$$T_D(Z,t) = T_{Do}\,\Delta r\left[-\alpha(Z) - \frac{2\pi r_B h_f}{GC_p}\beta(Z) + \frac{4\pi^2 r_D r_B U h_f}{G^2 C_p^2}\beta(Z)\frac{\beta(L)}{\alpha(L)}\right] - \frac{4\pi^2 r_D r_B U h_f}{G^2 C_p^2}$$

$$\int_0^Z T_f(Z-\tau,t)\,\Delta r \beta(\tau)d\tau = \frac{4\pi^2 r_D r_B U h_f}{G^2 C_p^2}$$

$$\Delta r\,\frac{\beta(Z)}{\alpha(L)}\int_0^L T_f(Z-\tau,t)\alpha(\tau)d\tau \quad , \quad . \quad (7)$$

and

$$T_A(Z,t) = T_D(Z,t) + \frac{2\pi r_B h_f}{GC_p}T_{Do}\,\Delta_r$$

$$\left[\beta(Z) - \frac{\alpha(Z)}{\alpha(L)}\beta(L)\right] + \frac{2\pi r_B h_f}{GC_p}\Delta r$$

$$\left[\int_0^Z T_f(Z-\tau,t)\,\alpha(\tau)d\tau - \frac{\alpha(Z)}{\alpha(L)}\right.$$

$$\left.\int_0^L T_f(Z-\tau,t)\,\alpha(\tau)\,d\tau\right] \quad . \quad . \quad . \quad . \quad . \quad (8)$$

The function $T_f(t,Z)_{r=r_B}$ is obtained as before (for the unsteady state) by solving the radial diffusivity equation and matching thermal fluxes between the annulus and the formation.

Solutions for transient profiles are much easier to obtain in the pseudo-steady state case since no time-step limitations are imposed by the numerical solution of the drill-pipe and annular temperature equations. The results from the unsteady state and pseudo-steady state cases are compared in Fig. 7. After 4 hours of circulation time, the temperatures calculated from the pseudo-steady state equations are nearly identical with those calculated from the unsteady state equations. Such results indicate that the pseudo-steady state model is adequate for calculation of temperature profiles for long circulation times. If the very early temperature behavior is desired, then the unsteady state solution must be used.

Temperature Behavior During Trip. The static fluid system approaches the geothermal gradient quite rapidly. In all simulated wells studied, only 16 hours were required for the fluid temperature to be within 10 percent of the geothermal temperature.

When a trip is started, fluid circulation is stopped and the fluid becomes quiescent in the borehole; at the end of a trip, fluid circulation is resumed. Experience in drilling deep wells has indicated that during a trip some parts of the fluid column in the borehole may be subjected to temperatures nearly equal to geothermal. The second phase of this study was directed toward simulating the thermal conditions that the fluid in the borehole experiences during a trip.

Since there is no forced convection during a trip, the major mode of heat transfer is either free convection or conduction in the fluid and conduction in the formation. Generally, the volume of fluid in the wellbore is extremely small compared with the volume of formation whose temperature is affected by circulation. Hence the conduction of heat in the fluid can be neglected. Also, an analysis of the system shows that free convection is negligible (Grashof number is much too small). Consequently, the temperature levels during the trip can be approximated by the conduction of heat in the formation, assuming that the fluid temperature is equal to the formation temperature at the borehole wall. Thus the radial diffusivity equation, Eq. 3, can be used to simulate temperature behavior during trips. To solve Eq. 3, an initial condition is necessary. For this purpose the temperature distribution in the formation at the conclusion of circulation is adequate.

Fig. 8 shows the temperature trace (borehole temperature vs time) for four different depths in the same system we used to calculate Figs. 2 through 6. As would be expected, at 5,000 ft circulation causes the formation to be heated slightly (30F) and then cooled. (The shape of this curve is similar to that of the surface temperature.) At 10,000 ft, very little temperature change takes place. At 20,000 ft, the temperature drops drastically (130F) and then heats up rapidly during a trip.

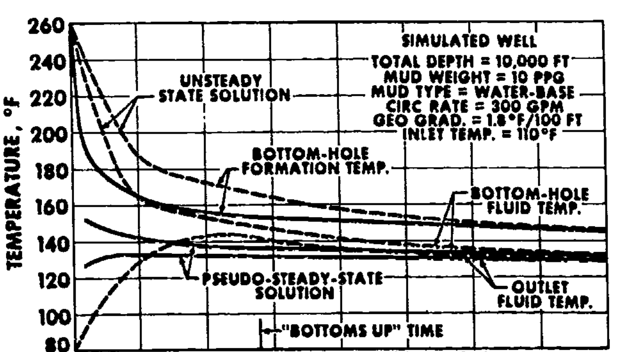

Fig. 7—Comparison of unsteady state and pseudo-steady state solutions.

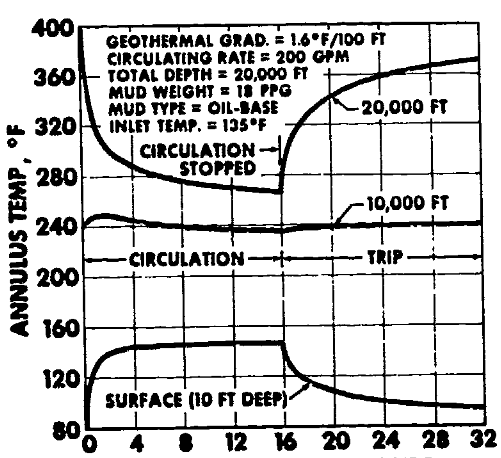

Fig. 8—Temperature trace for various depths in a simulated well.

Fig. 9 is a plot of percent of fluid above a given temperature vs temperature for the same 20,000-ft well. At the end of circulation, $t_{trip} = 0$, no fluid is above 270F, and all fluid in the wellbore is above 140F. As trip time increases, the profile rotates because the quiescent fluid at the top of the hole cools and the fluid at the bottom of the hole is heated. After just 1 hour of trip time, the maximum fluid temperature has increased to 310F and 35 percent of the fluid is above 270F. If the trip were very long (30 to 40 hours), the fluid's temperature distribution would approach geothermal (hence, the line for $t_{trip} = \infty$). The results in Fig. 9 are similar to those obtained in all other cases computed. For any trip longer than 16 hours, the fluid's temperature distribution is close to geothermal. The calculations indicate that formation beyond 10 ft from the wellbore was not affected significantly (less than 1 percent from original geothermal) during either the circulation or the trip.

Parameters Affecting Bottom-Hole Fluid Temperatures During Circulation

To assess the importance of each of the physical parameters in the system on the bottom-hole fluid temperature, a parametric sensitivity study was executed. It was found that the most important variables in the system were circulating rate, mud type (oil or water-base), and depth. The variable to which the bottom-hole fluid temperature was most sensitive was circulating rate. This is demonstrated in Fig. 10, where the difference between bottom-hole fluid temperature and outlet fluid temperature is plotted vs circulating rate Q for total depths of 10,000 and 20,000 ft.

Changes in geothermal gradient, as long as the gradient remains between 1.4F/100 ft and 2F/100 ft, have little effect on the temperature difference between bottom-hole fluid and other fluid for a 10,000-ft well (Fig. 11). In the 20,000-ft well of Fig. 11, the geothermal gradient had more effect on this temperature difference. The sensitivity to geothermal gradient was checked for several other muds at several depths, and similar results were obtained.

Fig. 12 shows that the effect of mud type and mud weight on ΔT — $T_A(L)$ or $T_D(L) - T_{outlet}$ — is a function of the total depth. By comparing Figs. 13 through 16 it can also be seen that the influence of mud weight on ΔT varies with the circulating rate. However, regardless of the depth or circulating rate, the ΔT for an oil-base mud was found to be greater than ΔT for an equivalent water-base system.

A study of hole size and drill-pipe size showed that as long as these dimensions remained within 30 percent of 8⅝ in. and 4½ in., respectively, there was no appreciable change in ΔT. Also, small changes

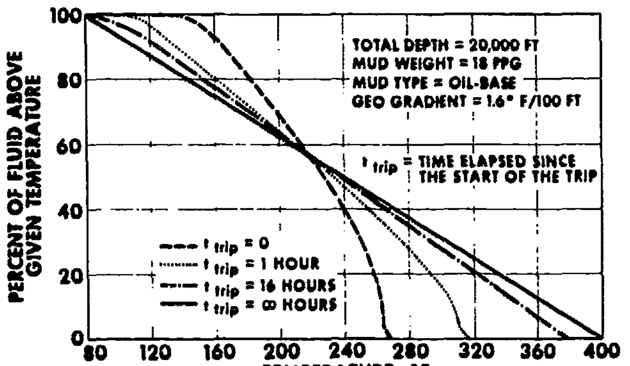

Fig. 9—Plot of percent of fluid above a given temperature vs temperature.

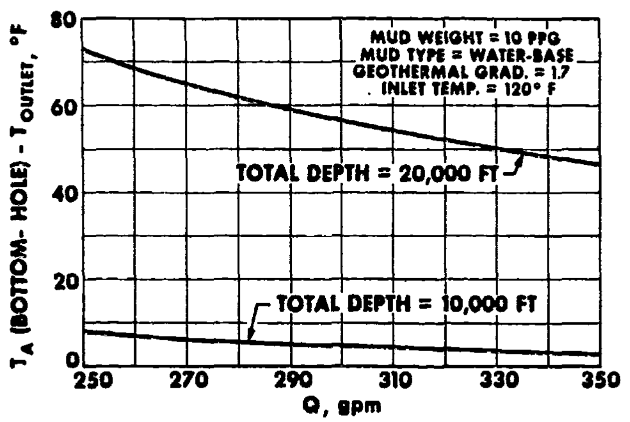

Fig. 10—Difference between bottom-hole fluid and outlet fluid temperatures vs circulating rate.

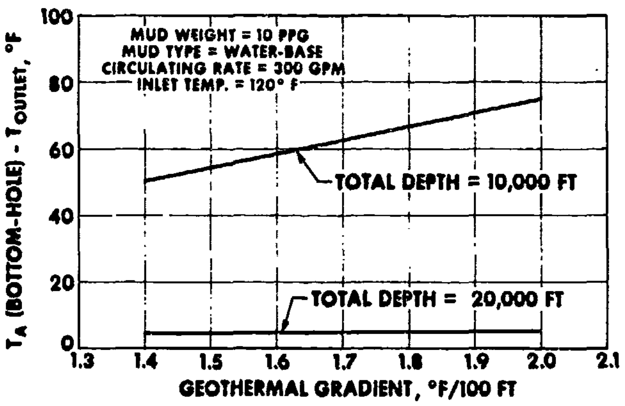

Fig. 11—Difference between bottom-hole fluid and outlet fluid temperatures vs geothermal gradient.

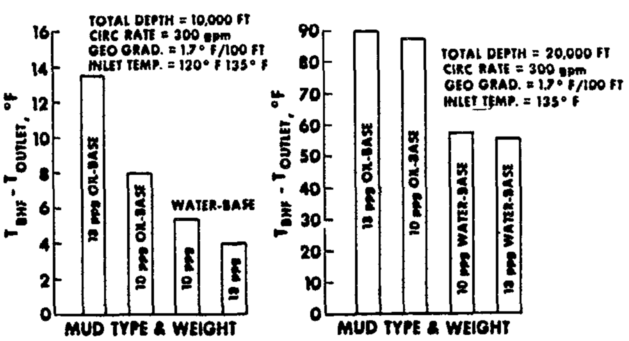

Fig. 12—Effect of mud type and mud weight on the difference between bottom-hole fluid and outlet fluid temperatures.

in the inlet temperature did not appreciably alter ΔT. In generating Figs. 12 through 16, the inlet temperature was held constant. For 10,000-ft wells, T_{Do} was 120F and for 25,000-ft wells, T_{Do} was 142.5F. T_{Do} for intermediate depths was obtained by linear interpolation between these two values.

Predicting Bottom-Hole Fluid Temperatures During Circulation

The circulation in over 70 wells was simulated to generate charts of ΔT vs Q for oil- and water-base muds. An important practical application of these charts is in predicting bottom-hole fluid temperature from a measured outlet temperature. Although the charts assume a geothermal gradient of 1.7F/100 ft, 4½-in. drill pipe, and a hole size of 8⅝ in., the results of the sensitivity study reveal that the charts can be applied to other conditions with reasonable confidence*; that is, pipe and hole size have little effect on circulating temperatures.

The results of these calculations are shown in Figs. 13 through 16. The ΔT plotted here is for a time after enough circulation has taken place so that bottoms have "come up" and a pseudo-steady state exists in the system. The charts can be used with accuracy if the inlet temperature is within 20F of the value used in the calculations.

*A cased hole should be treated the same as an open hole of like diameter. Geothermal gradient does not have much effect on predicted temperatures for depths to 10,000 ft (see Fig. 11). For best results below 10,000 ft, the actual geothermal gradient should be known. A correction can then be estimated from the right-hand graph of Fig. 11 (depth interpolation is reliable).

How to Use Charts

To predict the bottom-hole fluid temperature of a field well, record the outlet temperature, circulating rate, mud weight, and depth after 5 to 6 hours of circulation. Then use the charts in Figs. 13 through 16 to predict the bottom-hole fluid temperature for the proper mud type, as follows:

1. If the mud type is oil, use Figs. 13 and 14 to predict ΔT. If the mud type is water, use Figs. 15 and 16 to predict ΔT.
2. Use the depth of the well and the circulating rate to enter the ΔT vs Q charts; find the ΔT for 10 lb/gal and 18 lb/gal muds by linear interpolation for depth on the charts.
3. Interpolate the results from Step 2 for correct mud weight.
4. Add this ΔT to outlet temperature.

Example Problem

Fluid has been circulated at 280 gal/min for 6 hours

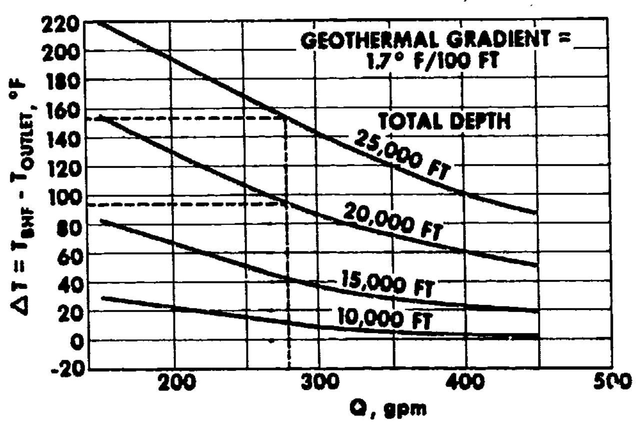

Fig. 13—Difference between bottom-hole fluid and outlet fluid temperatures for 10 lb/gal oil-base mud.

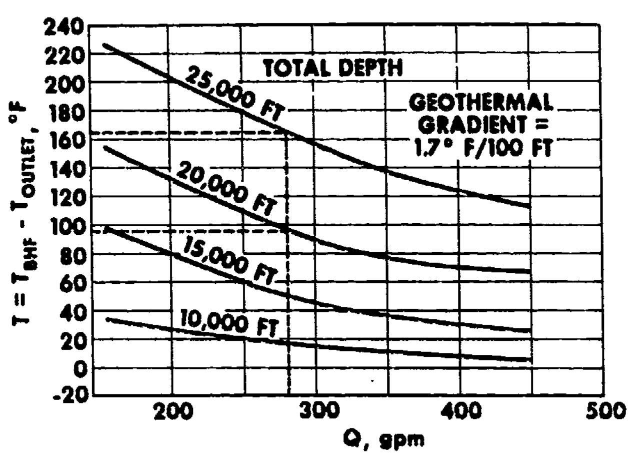

Fig. 14—Difference between bottom-hole fluid and outlet fluid temperatures for 18 lb/gal oil-base mud.

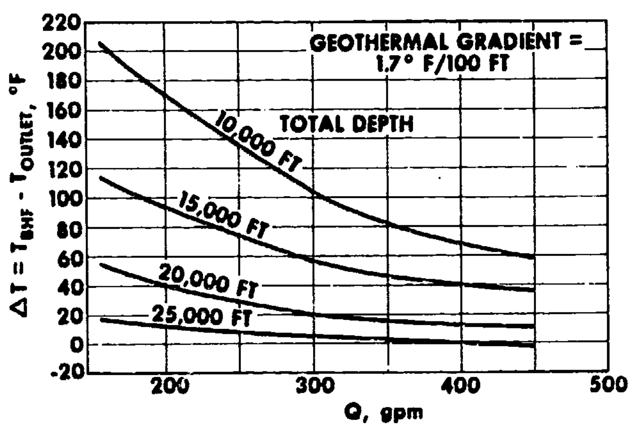

Fig. 15—Difference between bottom-hole fluid and outlet fluid temperatures for 10 lb/gal water-base mud.

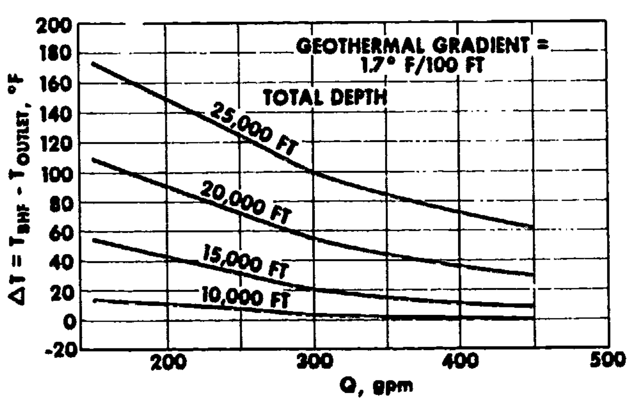

Fig. 16—Difference between bottom-hole fluid and outlet fluid temperature for 18 lb/gal water-base mud.

in a 22,400-ft well using a 15 lb/gal oil-base mud. The outlet temperature is 146.5F. What is the bottom-hole fluid temperature?

Enter the chart for $Q = 280$ (Fig. 13) and read

$\Delta T_{20{,}000\,ft} = 94F$;

$\Delta T_{25{,}000\,ft} = 153F$.

This is shown by the dotted lines on Fig. 13. Then by interpolation,

$$\Delta T_{22{,}400} = \Delta T_{20{,}000} + \left(\frac{22{,}400 - 20{,}000}{25{,}000 - 20{,}000}\right) \left(\Delta T_{25{,}000} - \Delta T_{20{,}000}\right) = 122F \text{ for a 10 lb/gal}$$

oil-base mud.

Similarly, enter Fig. 14 (see dotted lines) and obtain $\Delta T_{22{,}400} = 129F$ for an 18 lb/gal oil-base mud. Then, by interpolation again,

$$\Delta T_{22{,}400,\,15\,lb/gal} = \Delta T_{22{,}400,\,10\,lb/gal} + \frac{15\text{-}10}{18\text{-}10} (\Delta T_{22{,}400,\,18\,lb/gal} - \Delta T_{22{,}400,\,10\,lb/gal}) = 126F.$$

Thus the bottom-hole fluid temperature is 126 + 146.5 = 272.5F. The maximum fluid temperature (which occurs in the annulus at about 18,000 ft) is approximately 290F.

Conclusions

A technique to predict bottom-hole fluid temperatures in a circulating fluid system has been developed. The following conclusions have been reached in developing the technique.

1. During circulation, bottom-hole fluid temperature is *much* lower than the geothermal rock temperature.
2. Maximum fluid temperature in the circulating system occurs one-fourth to one-third of the way up the annulus.
3. All temperatures in the circulating fluid system change with time; a true steady state is never attained. However, after one or two mud circulations the temperatures do not change appreciably.
4. During trips, the fluid system tends quite rapidly toward the geothermal gradient. In all the wells studied, the fluid temperature distribution as a function of depth is within 10 percent of the geothermal gradient after 16 hours of trip time.
5. Large temperature gradients in the formation adjacent to the lower portion of the wellbore are established during circulation. The temperature of the formation 10 ft from the wellbore is essentially undisturbed during the drilling process.

Nomenclature

A_A = cross-sectional area of annulus
A_D = cross-sectional area of drill pipe
C_p = heat capacity of fluid
C_{pf} = heat capacity of formation
G = mass velocity
h_f = borehole wall heat transfer coefficient
k_f = formation thermal conductivity
L = total depth of well
Δr = variable defined in Appendix
r = radial space variable
r_B = borehole radius
r_D = drill-pipe radius
r_w = wellbore radius
v_A = annular fluid velocity
v_D = drill-pipe fluid velocity
$\Delta T = T_{\text{bottom-hole fluid}} - T_{\text{outlet}}$
T_A = annular temperature
T_D = drill-pipe temperature
T_f = formation temperature
T_{Do} = inlet drill-pipe temperature
U = over-all heat transfer coefficient between drill pipe and annulus
Z = depth variable
t = time variable
Δt = time step variable
α = variable defined in Appendix
β = variable defined in Appendix
ρ = fluid density
ρ_f = formation density
μ = fluid viscosity

References

1. Annis, M. R.: "High-Temperature Flow Properties of Water-Base Drilling Fluids", *J. Pet. Tech.* (Aug., 1967) 1074-1080.
2. Edwardson, M. J., Girner, H. M., Parkison, H. R., Williams, C. D. and Matthews, C. S.: "Calculation of Formation Temperature Disturbances Caused by Mud Circulation", *J. Pet. Tech.* (April, 1962) 416-426.
3. Farris, R. Floyd: "A Practical Evaluation of Cements for Oil Wells", *Drill. and Prod. Prac.*, API (1941) 283.
4. Tragesser, A. F., Crawford, P. B. and Crawford, H. R.: "A Method for Calculating Circulating Temperatures", *J. Pet. Tech.* (Nov., 1967) 1507-1512.
5. Polyakov, G. G.: "The Effect of Flushing on the Temperature in a Borehole During Drilling", *Izv. Vyssh. uncheb. Zavedenii Neft' i gaz* (1965) No. 9, 31.
6. Bird, R. B., Stewart, W. E. and Lightfoot, E. N.: *Transport Phenomena,* John Wiley & Sons, Inc., New York (1960).
7. Sieder, E. N. and Tate, G. E.: "Heat Transfer and Pressure Drop of Liquids in Tubes", *Ind. and Eng. Chem.* (1936) 1429.
8. van Everdingen, A. F. and Hurst, W.: "The Application of the Laplace Transformation to Flow Problems in Reservoirs", *Trans.,* AIME (1949) **186,** 305-324.

APPENDIX

Mathematical Model and Treatment

Discussion of Mathematical Model

The circulation of fluid during the drilling operation has been represented schematically in Fig. 1, and the process of circulation has been separated into three distinct phases: (1) fluid enters the drill pipe at the surface and passes down the drill pipe; (2) fluid exits the drill pipe through the bit and enters the annulus at the bottom; and (3) fluid passes up the annulus and exits the annulus at the surface.

The following assumptions are made to obtain the desired differential equations.

1. Axial conduction of heat in the fluid is negligible compared with axial convection. This is an excellent assumption for the circulating rates normally encountered in the circulation of drilling mud.
2. There are no radial gradients in the fluid in either

the drill pipe or the annulus. Since the fluid is in turbulent flow in the drill pipe and well mixed every 90 ft in the annulus because of tool joints and drill collars, this also is an excellent assumption.

3. The fluid's properties (heat capacity, density, and thermal conductivity) do not change significantly with temperature.

4. Heat generation by viscous dissipation in the fluid is negligible.

In the first phase, the fluid enters the drill pipe at a specified temperature, T_{Do}. As the fluid passes down the pipe, its temperature is determined by the rates at which (1) heat is convected down the drill pipe, (2) heat is exchanged between the drill pipe and the annulus, and (3) the temperature of the drill-pipe fluid changes with time. Consequently, the equation that describes the temperature of the fluid in the drill pipe as a function of time, t, and depth, Z, is

$$A_D \rho v_D C_p \frac{\partial T_D(Z,t)}{\partial Z} + 2\pi r_D U [T_D(Z,t) - T_A(Z,t)] = -\rho A_D C_p \frac{\partial T_D(Z,t)}{\partial t} \quad . \; . \; (1)$$

In Eq. 1 it has been assumed that the over-all heat transfer coefficient, U, is independent of depth and time. Since it has been previously assumed that the fluid properties are independent of temperature, this is a good assumption. The second phase of the circulating process merely requires that the fluid temperature at the exit of the drill pipe be the same as the fluid temperature at the entrance of the annulus; i.e., $T_D(L,t) = T_A(L,t)$. Thus, in the third phase the fluid enters the annulus at $T_D(L,t)$. As the fluid flows up the annulus, its temperature is determined by the rates at which (1) heat is convected up the annulus, (2) heat is exchanged between the annulus and the drill pipe, (3) heat is exchanged between the formation adjacent to the annulus and the fluid in the annulus, and (4) the temperature of the annular fluid changes with time. Consequently, the equation that describes the temperature of the fluid in the annulus as a function of t and F is

$$A_A \rho v_A C_p \frac{\partial T_A(Z,t)}{\partial Z} + 2\pi r_D U [T_D(Z,t) - T_A(Z,t)] + 2\pi r_B h_f [T_f(r_w,Z,t) - T_A(Z,t)] = \rho A_A C_p \frac{\partial T_A(Z,t)}{\partial t} \quad . \; . \; (2)$$

Since the thermal conductivity of the formation adjacent to the wellbore is small, it will be assumed that there is no transfer of heat by conduction in the vertical direction in the formation. Hence, the formation temperature $T_f(r_w,Z,t)$ is controlled by the radial diffusivity equation,

$$\frac{\partial T_f(r_w,Z,t)}{\partial t} = \frac{k_f}{\rho_f C_{pf}} \frac{1}{r} \frac{\partial}{\partial r}\left[r \frac{\partial T_f(r_w,Z,t)}{\partial r}\right] \quad . \; . \; . \; . \; . \; . \; . \; . \; . \; . \; . \; (3)$$

Eq. 3 is coupled with Eq. 2 through the rate of heat transfer between the fluid in the annulus and the formation. This requires that the flux of heat out of the formation be the same as the flux of heat into the annulus; that is, at any depth Z,

$$2\pi r_B h_f [T_f(t) - T_A(t)] = 2\pi r_B k_f \left[\frac{\partial T_f(t)}{\partial r}\right]_{r=r_B} \quad . \; . \; . \; . \; . \; . \; . \; . \; (4)$$

Hence, the temperature profiles in the drill pipe, annulus, and formation can be obtained by solving Eqs. 1 through 3, with the additional requirement specified by Eq. 4 once appropriate initial and boundary conditions are specified.

Numerical Method for Unsteady State Conditions

The transient temperature profiles used in this report are obtained as follows:

1. Using the specified circulating conditions, physical dimensions of the system, and fluid properties, calculate the heat transfer coefficients h_f and U from the Sieder-Tate[7] correlation.

2. Using the initial condition (geothermal temperature) $t = 0$, calculate the drill-pipe and annular temperature profiles at $t = \Delta t$ by solving Eqs. 1 and 2 by explicit finite differences. The formation temperature, $T_f(r_w, t, Z)$, used in the first step of the calculations is the geothermal temperature at depth Z.

3. From the calculated annular profile, calculate the flux of heat into the annulus from the formation.

4. Based on the flux just found, calculate the formation temperature, $T_f(r_w, \Delta t, Z)$, using the Hurst-van Everdingen P_{td} functions.[8]

5. Using this value of T_f, calculate the drill-pipe and annular temperature profiles, the flux, and the formation temperature. This iterative procedure is continued until the flux or formation temperature does not change significantly with iteration number.

6. At the next time step, Δt_2, use the previous values of the heat flux between the annulus and formation, and the principle of superposition, to predict $T_f(r_w, \Delta t_1 + \Delta t_2, Z)$. Then the drill-pipe and annular temperature profiles are calculated as before, and the iteration is continued until the calculations converge for $t = \Delta t_1 + \Delta t_2$.

7. This process is continued until the calculations are completed for the total circulation time, t_T.

Through this process the profiles are generated for transient drill-pipe temperature, annular temperature, and borehole wall temperature.

Solution of Pseudo-Steady State Condition

Consider the problem given by Eqs. 5 and 6 at any time, t. At this time there is a borehole wall temperature distribution $T_f(Z,t)$. The boundary conditions are:

$$T_D(Z=0,t) = T_{Do}$$

$$T_D(Z=L,t) = T_A(Z=L,t),$$

where T_{Do} is the inlet temperature and is assumed constant only for mathematical convenience.

Take the Laplace transform of Eqs. 5 and 6 to obtain

$$S\overline{T}_D + \frac{2\pi r_D U}{GC_p}(\overline{T}_D - \overline{T}_A) = T_{Do}\,, \quad \text{(A-1)}$$

and

$$S\overline{T}_A + \frac{2\pi r_D U}{GC_p}(\overline{T}_D - \overline{T}_A) + \frac{2\pi r_B h_f}{GC_p}[\overline{T}_f(t) - \overline{T}_A] = T_{Ao}\,, \quad \text{(A-2)}$$

where T_{Ao} is the outlet temperature from the annulus, S is the Laplace transform variable, and $G = \rho V_A A_A = \rho V_D A_A$. To meet the boundary condition at $Z = L$, T_{Ao} must be chosen such that $T_D(L,t) = T_A(L,t)$. Eqs. A-1 and A-2 are a set of algebraic equations that must be solved for $\overline{T}_D$ and $\overline{T}_A$. Using Cramer's rule, one obtains

$$\overline{T}_D = ST_{Do} + \frac{2\pi r_D U}{GC_p}T_{Ao} - \left(\frac{2\pi r_D U}{GC_p} + \frac{2\pi r_B h_f}{GC_p}\right) T_{Do} - \frac{4\pi^2 r_D r_B h_f U}{G^2 C_p^2}\overline{T}_f \Big/ \left(S + \frac{2\pi r_D U}{GC_p}\right)\left(S - \frac{2\pi r_D U}{GC_p} - \frac{2\pi r_B h_f}{GC_p}\right) + \frac{4\pi^2 r_D^2 U^2}{G^2 C_p^2} \quad \text{(A-3)}$$

and

$$\overline{T}_A = ST_{Ao} - \frac{S2\pi r_B h_f}{GC_p}\overline{T}_f + \frac{2\pi r_D U}{GC_p}(T_{Ao} - T_{Do}) - \frac{4\pi^2 r_B r_D h_f U}{G^2C_p^2}\overline{T}_f \Big/ \left(S + \frac{2\pi r_D U}{GC_p}\right)\left(S - \frac{2\pi r_D U}{GC_p} - \frac{2\pi r_B h_f}{GC_p}\right) + \frac{4\pi^2 r_D^2 U^2}{G^2C_p^2} \quad \text{(A-4)}$$

Note that the denominator in each of Eqs. A-3 and A-4 is a quadratic equation in the transform variable, S. Hence, Eqs. A-3 and A-4 can be inverted (with the roots of the quadratic) to obtain the temperature profiles. These roots are

$$r_{1,2} = -\left(\frac{\pi r_B h_f \pm \sqrt{\pi^2 r_B^2 h_f^2 + \pi^2 r_B r_D h_f U}}{GC_p}\right). \quad \text{(A-5)}$$

Thus

$$T_D(Z,t) = -T_{Do}\,\alpha(Z)\,\Delta r + \left[\frac{2\pi r_D U}{GC_p}T_{Ao} - \left(\frac{2\pi r_D U}{GC_p} + \frac{2\pi r_B h_f}{GC_p}\right)T_{Do}\right]\Delta r\beta(Z) - \frac{4\pi^2 r_D r_B h_f U}{G^2C_p^2}\int_0^Z T_f(Z-\tau,t)\,\Delta r\,\beta(\tau)d\tau, \quad \text{(A-6)}$$

where

$$\Delta = 1/(r_1 - r_2)\,,$$
$$\alpha(Z) = r_2 e^{-r_2 Z} - r_1 e^{-r_1 Z}\,,$$
$$\beta(Z) = e^{-r_2 Z} - e^{-r_1 Z}\,.$$

Similarly,

$$T_A(Z,t) = -\alpha(Z)\,T_{Ao}\,\Delta r + \frac{2\pi r_D U}{GC_p}\Delta r\beta(Z)(T_{Ao} - T_{Do}) + \frac{2\pi r_B h_f}{GC_p}\int_0^Z T_f(Z-\tau,t)\Delta r\alpha(\tau)d\tau - \frac{4\pi^2 r_B r_D U h_f}{G^2C_p^2}\int_0^Z T_f(Z-\tau,t)\,\Delta r\beta(\tau)d\tau\,. \quad \text{(A-7)}$$

From Eqs. A-6 and A-7, T_{Ao} can be chosen such that $T_A(L,t) = T_D(L,t)$. This requires

$$T_{Ao} = \frac{2\pi r_B h_f}{GC_p\alpha(L)}\int_0^L T_f(Z-\tau,t)\alpha(\tau)d\tau + T_{Do}\left(1 + \frac{2\pi r_B h_f\beta(L)}{GC_p\,\alpha(L)}\right). \quad \text{(A-8)}$$

Hence, relationships for $T_A(Z,t)$ and $T_D(Z,t)$ can be obtained in terms of Z, t, and the inlet temperature, T_{Do}.

$$T_D(Z,t) = T_{Do}\Delta r\left[-\alpha(Z) - \frac{2\pi r_B h_f}{GC_p}\beta(Z) + \frac{4\pi^2 r_D r_B U h_f}{G^2C_p^2}\beta(Z)\frac{\beta(L)}{\alpha(L)}\right] - \frac{4\pi^2 r_D r_B U h_f}{G^2C_p^2}\int_0^Z T_f(Z-\tau,t)\Delta r\beta(\tau)d\tau + \frac{4\pi^2 r_D r_B U h_f}{G^2C_p^2}\Delta r\frac{\beta(Z)}{\alpha(L)}\int_0^L T_f(Z-\tau,t)\alpha(\tau)d\tau \quad \text{(A-9)}$$

$$T_A(Z,t) = T_D(Z,t) + \frac{2\pi r_B h_f}{GC_p}T_{Do}\Delta r\left[\beta(Z) - \frac{\alpha(Z)}{\alpha(L)}\beta(L)\right] + \frac{2\pi r_B h_f}{GC_p}\Delta r\left[\int_0^Z T_f(Z-\tau,t)\alpha(\tau)d\tau - \frac{\alpha(Z)}{\alpha(L)}\int_L^0 T_f(Z-\tau,t)\alpha(\tau)d\tau\right]. \quad \text{(A-10)}$$

JPT

Original manuscript received in Society of Petroleum Engineers office June 4, 1968. Revised manuscript received Nov. 12, 1968. Paper (SPE 2320) was presented at SPE Symposium on Drilling and Rock Mechanics held in Austin, Tex., Jan. 14-15, 1969.

This paper will be printed in *Transactions* volume 246, which will cover 1969.